Reducing uncertainty in source area exploration of mineralized glacial erratics using terrestrial cosmogenic radionuclide dating

Veikko Peltonen, Seija Kultti, Niko Putkinen, Vincent Rinterknecht, Adrian Hall, David Whipp

Journal of Geochemical Exploration 261 (2024) 107456

Contents lists available at ScienceDirect

Journal of Geochemical Exploration

journal homepage: www.elsevier.com/locate/gexplo

Reducing uncertainty in source area exploration of mineralized glacial erratics using terrestrial cosmogenic radionuclide dating

Veikko Peltonen [a,*], Seija Kultti [a], Niko Putkinen [b], Vincent Rinterknecht [c], Adrian Hall [d], David Whipp [a]

[a] Deparment of Geosciences and Geography, University of Helsinki, Finland
[b] Geological Survey of Finland, Kokkola, Finland
[c] Aix Marseille Univ, CNRS, IRD, INRAE, CEREGE, Aix-en-Provence, France
[d] Institute of Geography, University of Edinburgh, Drummond Street, Edinburgh, UK

ARTICLE INFO

Keywords:
Mineral exploration
Drift prospecting
Terrestrial cosmogenic nuclide dating
Central Lapland Greenstone Belt
Glaciated terrain
Glacial erosion

ABSTRACT

Mineral exploration often relies on sedimentary indicators as first signs of a potential nearby mineralization in bedrock. The transportation of sediment by glacial and fluvial processes introduces uncertainty into the tracing of potential source areas of the sediment. This is particularly challenging in areas where glacial erosion has been weak, resulting in reworking of sediments and multiple directions of transportation. In this study we explore the use of Terrestrial Cosmogenic Nuclides (TCN) alongside conventional mineral exploration methods to better link indicators with their potential source areas.

The study focuses on a mineral exploration project site in northern Finland in a region with stratigraphic evidence of multiple glaciations. The project targets the source of discovered Au mineralized erratic boulders that have been deposited atop the most recent till unit. The superposition suggests transportation in the latest glacial event. However, the ^{10}Be (35.9 ± 1.3 and 30.3 ± 1.1 ka) and ^{26}Al TCN ages analyzed from the mineralized erratics precede the latest glacial event, suggesting the possibility of multiple stages of transportation. The local bedrock TCN inventories (48.9 ± 1.9 and 85.3 ± 2.8 ka) are well preserved, suggestive of weak glacial erosion and therefore short recent transportation distances for the mineralized erratics. By combining the TCN interpretation and historical ice flow directions derived from the till stratigraphy, we suggest a nearby source locating NNW of the dated erratics.

We find that TCN dating can limit some of the transportation related uncertainties in glaciated terrain. Through the analysis of TCN inventories from bedrock and boulders it is possible to characterize glacial erosion and boulder transportation, and to identify repeated exposure events, i.e., the possibility of multi-staged transportation. The method benefits from combined use of stratigraphic investigations that can identify both the local transportation directions and local glacial coverage history. TCN sampling has a minimal environmental impact, can be used in remote areas and can provide information about the transport history already in the early stages of exploration. Although the analysis is time consuming, the survey is light to conduct and informative even with a small number of samples.

1. Introduction

Sediments are a commonly used tool for identifying potential source areas of mineralized bedrock. The interpretation of how the sediment has been transported varies according to the sedimentary environment. In mineral exploration in glaciated terrain the possibility of transportation by various glacial, glacifluvial and fluvial processes needs to be accounted for. The sedimentary cover poses challenges for mineral exploration throughout the Northern Hemisphere and requires many greenfield and some brownfield projects to use different kinds of sediment sampling surveys in the search of mineral deposits. Till is generally accepted as a geochemical sampling medium in mineral exploration, although it contains inherit uncertainties that can make it difficult to trace the origin of anomalous samples (Nichol and Bjorklund, 1973; Levson and Giles, 1995). The difficulties are amplified in weakly erosive regions where the sediment cover can be complex and composed of

* Corresponding author at: Department of Geosciences and Geography, University of Helsinki, P.O. Box 64, Fi-00014, Finland.
E-mail address: veikko.peltonen@helsinki.fi (V. Peltonen).

https://doi.org/10.1016/j.gexplo.2024.107456
Received 9 January 2023; Received in revised form 30 May 2023; Accepted 13 March 2024
Available online 16 March 2024

multiple reworked till units (Hirvas, 1991; Lunkka et al., 2013).

Glaciers generate till by recycling underlying sediments and eroded bedrock, distributing this material along the movement direction of the glacier (cf. DiLabio, 1990, Aario and Peuraniemi, 1992 and McClenaghan and Paulen, 2017). Immature tills in which the local bedrock component is large can carry geochemical resemblance to their bedrock source. Such tills can contain geochemical trains or fans that can be traced back to their bedrock source (Bradshaw et al., 1974; Klassen and Gubins, 1997), typically following the most recent ice flow direction (McClenaghan et al., 2000).

However, if the till is mostly composed of previously eroded sediments (e.g., pre-existing tills), the transportation vector of the new till unit will reflect both the new transportation direction and the direction (s) of the pre-existing till. Such multi-staged transportation has been documented to complicate provenance tracing of erratics and geochemical samples within glaciated regions (e.g., Hirvas and Nenonen, 1990; Parent et al., 1996). However, in some cases, in particular in areas where glacial erosion has been repeatedly weak, the transportation path of erratics can be more complicated to decipher (Salonen, 1986). If the difficulty in erratic tracing derives from the erratic being transported in multiple glaciations, as concluded about parts of Central Finnish Lapland by Salonen (1986), the erratics and local bedrock could record indications of this in their TCN inventories. If so, TCNs could be used to identify the possibility of multi staged transportation already in the early stages of exploration.

One way to reduce uncertainty in the source areas of glacially transported sediment is to quantify the erosion and transportation history using terrestrial cosmogenic nuclides (TCN). TCNs are nuclides that are produced in rocks within a few meters of Earth's surface when they are exposed to secondary high-energy radiation from space (Dunai, 2010; Schaefer et al., 2022). TCN dating method uses the small but measurable concentrations of the cosmogenic radionuclides to estimate the exposure duration of rock samples**.** The usefulness of the method can be further broadened by measuring multiple radiogenic TCNs. TCNs such as ^{26}Al and ^{10}Be have a steady production rate ratio but differing half-lives. The ratio can record interruptions in exposure (Gosse and Phillips, 2001) and details of erosion events and surface erosion (Hall et al., 2019). Using two TCNs therefore provides the apparent exposure age like the single nuclide approach, but also insight on the erosion and exposure history i.e., reburial of the samples (Corbett et al., 2013). Thus, TCNs could be used to identify the possibility of multi staged transportation already in the early stages of exploration.

In this study we explore the potential benefits of adding TCN analysis to conventional exploration methods in tracing mineralization source areas. The study is conducted at an orogenic Au prospect in the Central Finnish Lapland. The region is perceived as being a weakly erosive ice divide area with high variability in sequential ice-flow directions (Kleman et al., 1997). It hosts active green and brownfield exploration (Niiranen et al., 2015) and is widely covered by a complex glacial sediment stratigraphy (Hirvas, 1991). The prospect at Kaarestunturi is based on the discovery of surficial Au mineralized quartz vein erratics. The source of the erratics is unknown, the erratics are autochthonous and locate on complex sediment beds. Tracing the erosion resistant and pathfinder element poor quartz veins in quartzite rich environment is challenging for geophysical and geochemical methods. The project is optimal for testing alternative methods for erratic tracing. For the study we measure the ^{10}Be and ^{26}Al TCN inventories of two mineralized quartz erratics and two local bedrock outcrops and document sediment stratigraphy from five machine cut trenches. The TCN and stratigraphic results are used to study local glacial history, erosion and transportation, and the exposure duration of the mineralized erratics. The TCN results and local glacial history studies provide new information on the possible source area of the mineralized erratics. Last, we discuss the wider applicability of TCN dating in exploration.

2. Study area

2.1. Geological setting

The Finnish central Lapland is both an historical and active region for mineral exploration. Currently the region's primary metal products are Au, Ni and Cu, from the Kittilä and the Kevitsa mines. The Finnish Central Lapland is mostly composed of the Paleoproterozoic Central Lapland Greenstone Belt (CLGB). The belt is seen as a host for orogenic gold deposits (Niiranen et al., 2015). CLGB resides mostly in a region of weak glacial erosion (Ebert et al., 2015) where the sediments widely cover the bedrock (Hirvas et al., 1977). Most of the bedrock outcrops can be found at topographical highs where resistant lithologies stand out as fells in the flat landscape. The study area at Kaarestunturi fell is mostly covered by till and boulder fields, and at low elevations peatland (Fig. 2B). Outcrops of the varying quartzites can be found on some of the peaks and slopes (Fig. 2A).

2A. TCN sampling sites, studied trenches and erratic quartz boulders. CRE-01 and CRE-02 are dated erratics and CRE-03 and CRE-04 are dated bedrock outrcops. AMT-1801 to AMT-1903 are studied trenches on the southern and eastern side of Kaarestunturi fell. The red line C-C′ marks conceptual cross section in Fig. 2B.

2B. Conceptual cross section C-C′ illustrates the topographic positions between the terrestrial cosmogenic nuclide samples and the general sediment stratigraphy south of the fell. The profile runs from a SE peak of the fell to the water table at the Kaareoja brook.

2.2. Glacial setting

Lapland has experienced up to five glacial advances in the last glacial cycle, c. 10–110 ka (Johansson et al., 2011). The cold period is referred to as the Weichselian in Scandinavia and it spans from Marine Isotope Stage (MIS) 2 to MIS-5d (Railsback et al., 2015). Ice did not advance across Finnish Lapland in every Weichselian stadial and the evidence of ice cover is more extensive in Western Lapland, closer to the glacial nucleation center (Helmens et al., 2000; Helmens and Engels, 2010; Lunkka et al., 2015)**.** Current evidence suggests that the study area in the Sodankylä municipality was glaciated between two and four times during the Weichselian glacial period (Salonen et al., 2008; Sarala and Eskola, 2011). Such uncertainty is characteristic to areas with continental glaciers. The evidences of earlier glaciations are often destroyed by younger glaciers, or buried underneath new glacigenic sediments. This leads to sparse observations and subsequently difficulties in establishing the local glacial chronology. The extent of the latest Weichselian glaciation are relatively well known (Hughes et al., 2016), but the extents of the earlier Weichselian ice advances are still uncertain at the study area (Sarala et al., 2015; Åberg et al., 2020; Sutinen and Middleton, 2021). Glacial events are significant to both the interpretation of the TCN ages (Corbett et al., 2013) and glacial transportation of geochemical indicators (Parent et al., 1996).

The historical glacial transportation directions within the CLGB have varied extensively. Near the study area the directions have varied from NW-SE during Early Weichselian to NNW-SSE in Middle Weichselian to SW-NE in Late Weichselian (Hirvas et al., 1977; Härkönen et al., 1981; Bouchard and Salonen, 1990; Hirvas, 1991; Kleman et al., 1997; Åberg et al., 2020). Sequential ice-flow events can rework glacigenic sediments, the reworking can create asynchronous dispersal fans and overprinting palimpsests (Parent et al., 1996). Establishing a connection between a reworked dispersal fan and its bedrock source can be difficult for exploration (McClenaghan et al., 2000), and particularly problematic if the reworked character of the dispersal fan is not recognized.

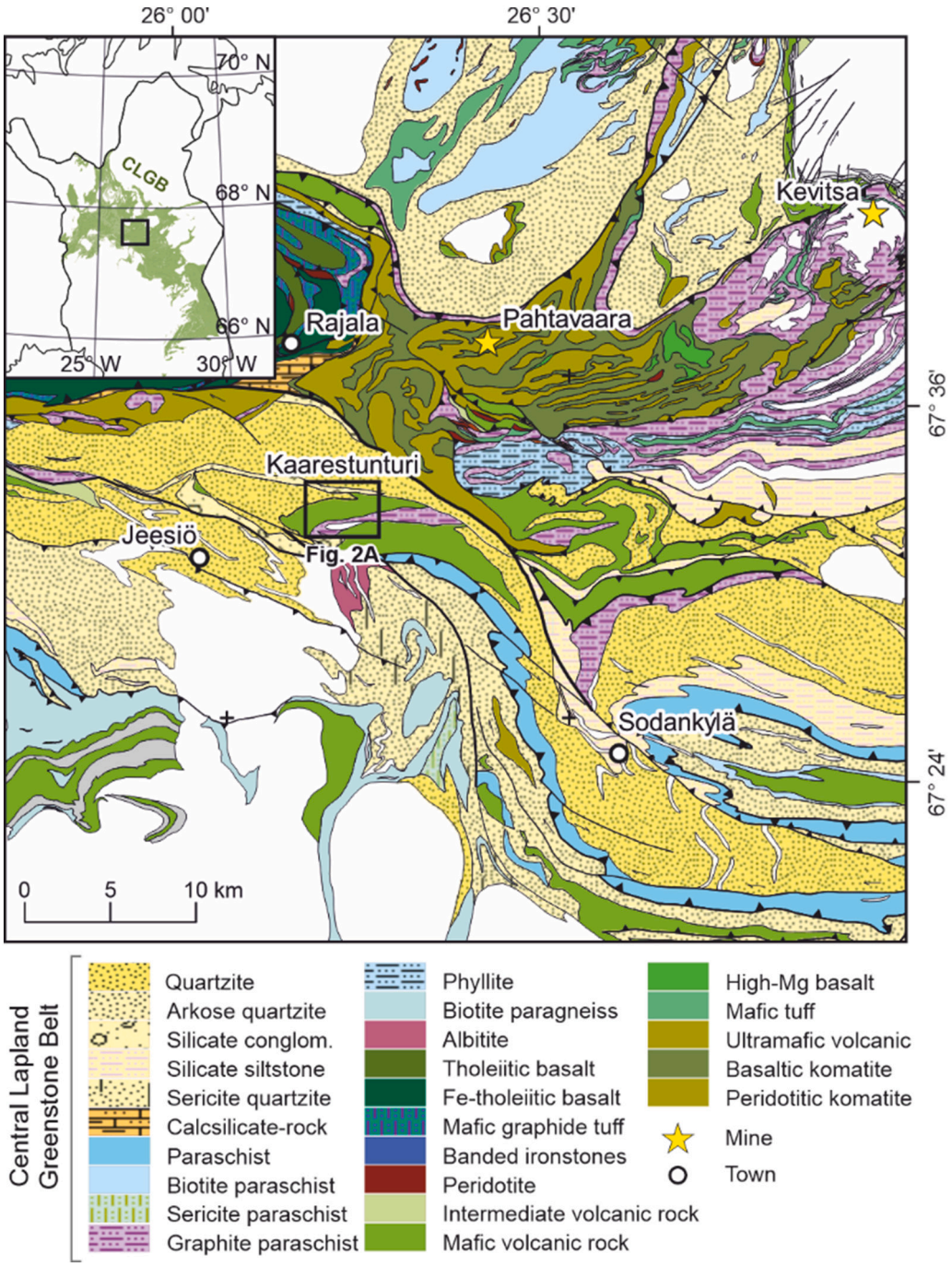

Fig. 1. A lithostratigraphic map of the Central Lapland Greenstone belt (CLGB). The CLGB rock types are color coded and the Archean basement and Paleoproterozoic intrusive units are presented in white. The study area of Kaarestunturi is marked with a box. Modified and reproduced from GTK's Bedrock of Finland 1:200,000 data, under GTK open license CC BY 4.0, imported from Hakku service on 1 December 2022.

3. Materials and methods

3.1. Terrestrial cosmogenic nuclide dating using ^{10}Be and ^{26}Al

3.1.1. TCN theory and data interpretation

Cosmogenic ^{10}Be and ^{26}Al are rare radioisotopes produced in-situ in specific minerals (primarily quartz) near the Earth's surface, due to irradiation by secondary high-energy particles (Davis Jr and Schaeffer, 1955; Lal and Peters, 1967). The principle in TCN-dating is that the concentration of the cosmogenic nuclides grows as a function of the time a sample has spent at or near the Earth's surface until the TCN inventory reaches secular equilibrium. Thus, higher concentrations generally mean longer exposure to the cosmogenic radiation flux. Due to the exponential attenuation of the (energy) flux in the crust, TCNs that are produced are most abundant in rock exposed at the surface (Fig. 3). At a depth of ~3 m, ^{10}Be production is already virtually null, and the behaviour of ^{26}Al is similar. Although surface exposure is a key factor affecting the concentrations of TCNs (i.e., the TCN inventory) in a sample, the concentration is also affected by several other factors, including: (1) the exposure duration (single, continuous exposure or complex multi-exposure histories in the case of intermittent shielding from cosmic rays); (2) the production rates at the site, which vary due to atmospheric shielding (altitude) and magnetic field effects (latitude); (3) site-specific factors such as snow, sediment and vegetation cover; (4)

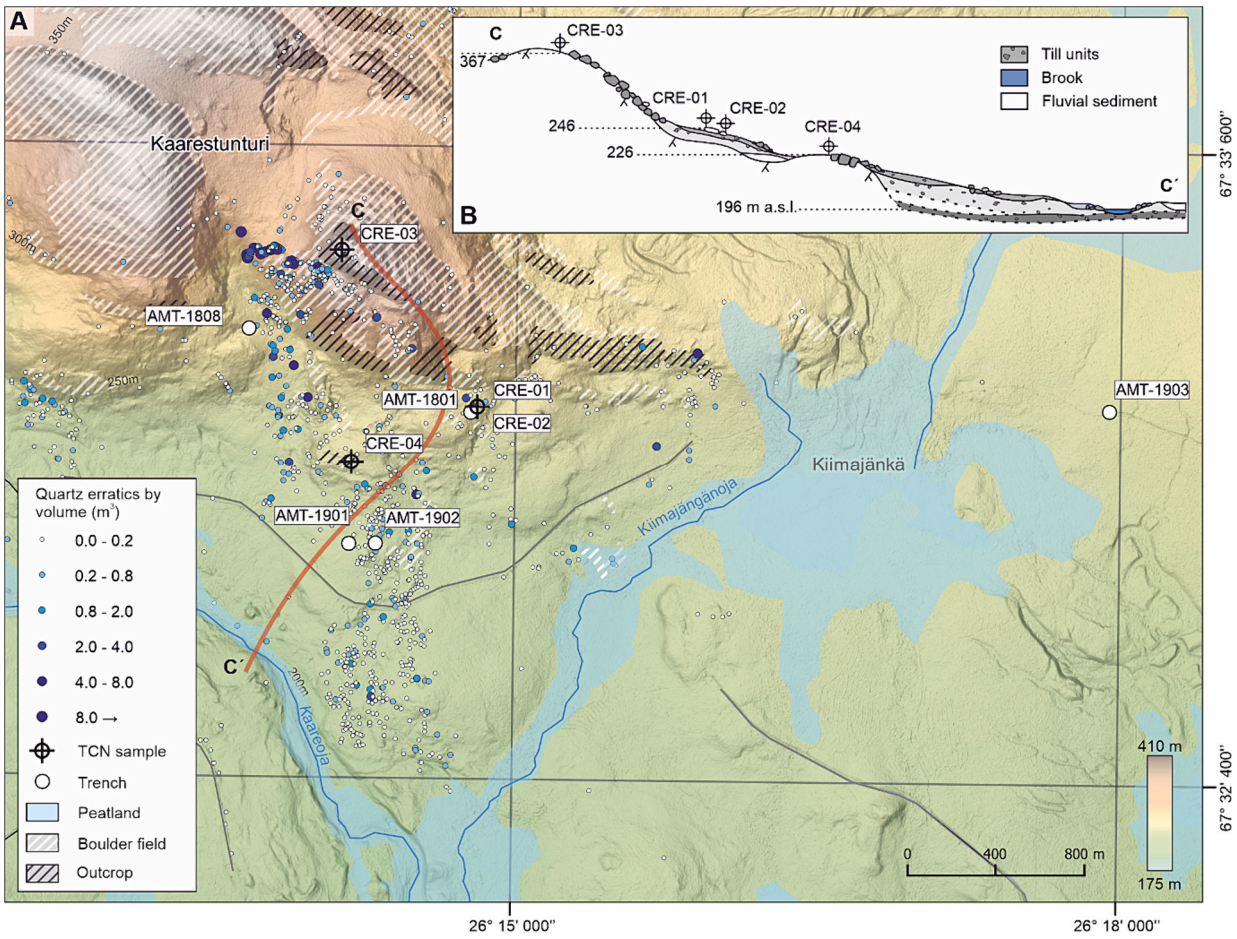

Fig. 2. Topography of the southern and eastern side of Kaaretunturi fell. Location indicated in Fig. 1. LiDAR DEM: © modified and reproduced after the National Land Survey of Finland, accessed on 1 December 2022.

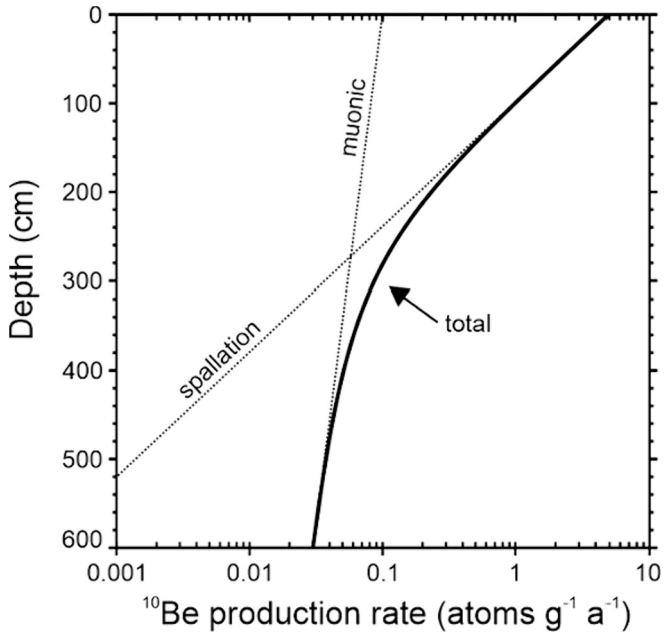

Fig. 3. ^{10}Be production as a function of depth in quartz arkose. Modified from Gosse and Phillips (2001).

surface erosion and removal of rock near the surface; and (5) the radioactive decay of the cosmogenic nuclides (Gosse and Phillips, 2001). Knowing or estimating the aforementioned factors allows estimation of the minimum exposure ages from the TCN inventories (i.e., dating them).

Because TCNs form at and near the surface, the existing TCN inventory of an outcrop surface can be fully removed when the erosion reaches depths of ~3 m. Such erosion may occur in a single highly erosive event, forming what termed an *event* surface (Phillips et al., 2006). Incomplete removal of the TCN inventory from less erosion, on the other hand, creates surfaces with inheritance (Corbett et al., 2013; Hilger et al., 2019; Andersen et al., 2020). Inheritance is common on tors and in former glacial ice divide regions where glacial erosion has been weak or non-existent. Inheritance allows TCN inventories to be used to quantify depths and rates of erosion (Margreth et al., 2014; Hall et al., 2019).

Measuring a single terrestrial cosmogenic nuclide suffices for samples and environments where the exposure history is expected to be continuous, however measurements of multiple TCNs can provide information about both the sample's exposure and burial history (Granger and Muzikar, 2001). The radionuclides ^{26}Al and ^{10}Be form at different rates and have different half-lives (1.4 Ma for ^{10}Be and 0.7 Ma for ^{26}Al (Chmeleff et al., 2010, Korschinek et al., 2010). Because burial disproportionally depletes the concentration of ^{26}Al compared to ^{10}Be, the ^{26}Al/^{10}Be ratio can be used as an indicator of complex exposure and burial history (Bierman et al., 1999; Corbett et al., 2013). However, the reliability of the ratio as a burial indicator rests on the knowledge of the local TCN production rate ratios during exposure. In nature ratios vary

spatially and temporally from 6.75 (Argento et al., 2015) to 7.3 at Arctic latitudes (Corbett et al., 2017).

3.1.2. TCN sample collection strategy

Four samples were collected from the southern side of the Kaarestunturi fell (Figs. 2, 4) following the guidelines in Gosse and Phillips (2001). Samples CRE-01 and CRE-02 were collected from gold bearing quartz-vein erratics, while samples CRE-03 and CRE-04 are from quartz arenite outcrops of the Kumpu group at a summit and the southern slope of the Kaarestunturi fell (Fig. 2A). The specific quartz-vein erratics were chosen due to their large size and tabular shape. The tabular erratics are likely to lay on either of the two faces. This mitigates some of the uncertainty that comes from the possible overturning or irregularly shaped boulders (Tylmann et al., 2019). As the possible overturning would only lead to underestimation of the ages so, the measured erratic TCN ages will be valid as minimum exposure ages.

We systematically collected all samples from minimally shielded horizontal or near horizontal surfaces using a rock saw, avoiding rounded or chipped edges in the process. Sample coordinates and elevations were recorded with a handheld GPS receiver and shielding by surrounding topographical slopes was recorded using a compass and a clinometer. The quartz content of the samples is >70 % (Table 1).

3.1.3. TCN sample preparation and analysis

The samples were prepared at the CALM (Cosmonucléides Au Laboratoire de Meudon) laboratory in France. We analyzed both ^{26}Al and ^{10}Be given the possibility of multiple exposure events. All samples were crushed and sieved to the 250–710 μm fraction. We used magnetic separation and mineral flotation techniques prior to chemical etching procedures modified from Kohl and Nishiizumi (1992) to separate and purify the quartz fraction. Quartz purity was assayed using ICP-OES. Up to 450 μl of a commercial ^{9}Be carrier (Scharlau) was added to each sample. Beryllium extraction was carried out using methods modified from Child et al. (2000). Beryllium isotope ratios in the samples and one procedural blank were measured at ASTER (the French Accelerator Mass Spectrometer located at CEREGE, Aix-en-Provence). Data were normalised directly against the National Institute of Standards and Technology (NIST) standard reference material 4325 using an assigned ^{10}Be/^{9}Be ratio of (2.79 ± 0.03) × 10^{-11} (Nishiizumi et al., 2007) and a ^{10}Be half-life of (1.387 ± 0.012) × 10^{6} years (Chmeleff et al., 2010; Korschinek et al., 2010). To ensure that enough ^{27}Al was present in the parental solution of all samples, aliquots of ~0.5 g were removed for ICP-OES analyses. Based on the results, up to 1200 μl of a commercial ^{27}Al carrier (Scharlau) was added to each sample. Aluminium isotope ratios in the samples and one procedural blank were measured at ASTER. Data were normalised directly against the in-house standard SM-Al-11 with an assigned ^{26}Al/^{27}Al ratio of (7.401 ± 0.064) x 10^{-12} (Arnold et al., 2010).

Analytical uncertainties (reported as one sigma) include a conservative 0.5 % uncertainty based on long-term measurements of standards, a one sigma statistical error on counted ^{10}Be and ^{26}Al events, and the uncertainties associated with the chemical and analytical blank correction; the ^{10}Be/^{9}Be blank ratio was 5.99 × 10^{-15} and the ^{26}Al/^{27}Al blank ratio was 1.80 × 10^{-15}.

Fig. 4. A drone photograph of the sampling site for CRE-01 and 02 quartz erratics. For location see Fig. 2. The diameter of the erratics is up to 2.5 m. The quartz erratics outlined in magenta were moved during excavation. Photo by Veikko Peltonen.

3.2. Quaternary stratigraphy and fabric measurements

The local stratigraphy was studied from five machine-cut trenches dug for ore exploration on the south and east sides of the Kaarestunturi fell. The trenches used for the study are AMT-1801, AMT-1808, AMT-1901, AMT-1902 and AMT-1903 (Fig. 2). The lithofacies codes take after Eyles et al. (1983). Seven fabric measurements were conducted in the trenches to study past ice flow directions. Each fabric calculation consisted of measuring the a-axis orientation of 25 clasts. Measured clasts were longer than 2 cm in length and have a- to b-axis ratios ≥2. Clasts that were disturbed by clast-to-clast contacts or proximal to large boulders were not measured.

3.3. Optically stimulated luminescence (OSL) measurement

One interbedded sand unit in trench AMT-1903, east of the fell was dated by OSL. Sample KJ-191 was collected from AMT-1903 at 4.2 m depth from within an interbedded sand unit. The sample was gathered by hammering a 5-cm PVC tube into an undisturbed, freshly cleaned section of the sediment crosscut and covering the sand-filled tube with foil after extraction. The on-site gamma dose radiation was measured with an ICx-IdentiFINDER digital gamma spectrometer with a 1.4″ × 2” NaI (Ti) detector. The gamma measurement included cosmic radiation. The actual gamma dose was calculated with an estimated water content of 20 % according to Aitken (1985). The analysis was conducted at the Luomus laboratory at the University of Helsinki. The target mineral for the OSL measurement was quartz, of which the 210–297 μm diameter size fraction was separated and etched with 40 % HF and 10 % HCl for 1 h and 30 min, respectively. The beta dose rate was measured with a Risø TL-DA-12 reader (Bøtter-Jensen and Duller, 1992; Bøtter-Jensen et al., 1999). The OSL sample preparation is described in more detail in Salonen et al. (2008).

3.4. Erratic sampling survey

The erratic sampling survey was conducted by the company Aurion Resources LTD as a routine step of mineral exploration on the tenure. The erratic dataset consists of 1238 quartz vein erratic samples from the site. The sample collection was done by hand and ultimately included most surficial quartz vein fragments found on the site. Documentation included approximating the size of the erratic/boulder and recording its location with a handheld GPS. Geochemical assays or mineral descriptions from the erratics are not used in this study.

4. Results

4.1. TCN inventories

We report here the sample minimum surface exposure ages based on the ^{10}Be and ^{26}Al concentrations and using the “St” scaling scheme (Stone, 2000). The scheme assumes constant nuclide production rates and does not account for variations in the magnetic field (Balco et al., 2008). In the exposure age calculations we used ^{10}Be and ^{26}Al production rates derived from the primary calibration dataset of Borchers et al. (2016) and version 3 of the online calculator formerly known as The

Table 1
TCN sample characteristics.

Sample	Sample type	Municipality	Latitude (DD)	Longitude (DD)	Elevation (m a.s.l.)	Sample thickness (cm)	Shielding correction	Density (g cm-3)
CRE-01	Erratic	Sodankylä	67.5517	26.2467	246	5	1	2.584
CRE-02	Erratic	Sodankylä	67.5517	26.2466	246	5	1	2.584
CRE-03	Outcrop	Sodankylä	67.5564	26.2357	367	4.6	0.998	2.745
CRE-04	Outcrop	Sodankylä	67.5498	26.2363	226	5	0.999	2.646

CRONUS-Earth online calculators (Balco et al., 2008). Due to limited information about past erosion rate and snow shielding, the results are presented both with and without those corrections (Tables 3 and 4). The modern vegetation in the northern boreal zone is light; a partial weak moss covered the sampled quartz erratics and the bedrock locations had no vegetation cover at the time of sampling. We consider the effect of vegetation shielding to be minimal and do not estimate corrections for it.

The apparent ^{10}Be ages of the CRE-01 and CRE-02 erratics are 37.8 ± 1.2 ka and 29.5 ± 1.0 ka, respectively. The ^{10}Be ages of the outcrop samples CRE-03 and CRE-04 are older, 50.3 ± 1.6 ka and 91.0 ± 2.4 ka, respectively. The ^{26}Al/ ^{10}Be ratios correlate nearly linearly with the exposure age, except for CRE-01 whose ^{26}Al/^{10}Be ratio of 6.48 deviates downwards. The ^{26}Al/^{10}Be production ratio resulting from the use of Borchers et al. (2016) production rates is ~7.0, slightly higher than the ~6.75 by Argento et al. (2015) but in line with what is suggested in Corbett et al. (2017).

4.2. Shielding- and erosion-corrected TCN exposure ages

The TCN inventory accumulation is consistently suppressed by snow shielding and reversed by surface erosion. According to the Finnish Meteorological Institute the modern average annual snow thickness in the region is 26 cm. We correct for the annual snow shielding by adding the snow cover as a virtual site-specific sample thickness and extrapolating it over the exposure history of the sample. Slightly thinner snow cover is assumed on the peak of the fell for CRE-03 (Fig. 2). We apply erosion rates from 0.5 to 0.9 mm ka^{-1} (Stroeven et al., 2002; Balco et al., 2014) to the samples according to their quartz richness. For the purpose of our discussion, we consider the corrected exposure ages to be the most representative exposure ages (Table 4).

4.3. Sediment stratigraphy

Five stratigraphic sections were logged from five machine cut trenches (AMT-1801–AMT-1903) on the study site (Figs. 2, 5). The trenches situate near and at locations where mineralized quartz vein erratics have been sampled. We observed total of 4 till units (abbreviated as TU-1–TU-4) and sorted sediment units. One sorted sediment was dated by OSL to being 79 ± 13 ka old, the sand unit is interbedded between the TU-1 and TU-2 till units in trench AMT-1903.

Till unit TU-1 is a matrix supported weakly packed diamicton. The unit composes of a sandy matrix and approximately 20 % clasts. Clasts mode is in the pebble size range. The fabric calculation produces a SSW-NNE orientated rose diagram. Till unit TU-2 is a clast supported moderately packed diamicton. The unit composes of up to boulder sized clasts with a mixed clay rich matrix. Clasts mode is in the boulder size range. Due to the clast supported nature of the unit, a fabric calculation was not possible. Till unit TU-3 is a matrix supported weakly packed diamicton. The unit composes of a sandy matrix and up to 70 % clasts. Clasts mode is in the boulder range. The unit hosts the largest boulders of all the observed till units. The till unit has a SSW-NNE fabric. The fabric was measured from two trenches (AMT-1901 and AMT-1903). A fabric measurement was conducted from a thin diamicton unit in between the TU-4 and TU-3 in AMT-1901, the rose diagram was incoherent. The unit itself is possibly a part of the TU-3 or TU-4 as it was not encountered in other trenches. Till unit TU-4 is a matrix-supported, very weakly packed

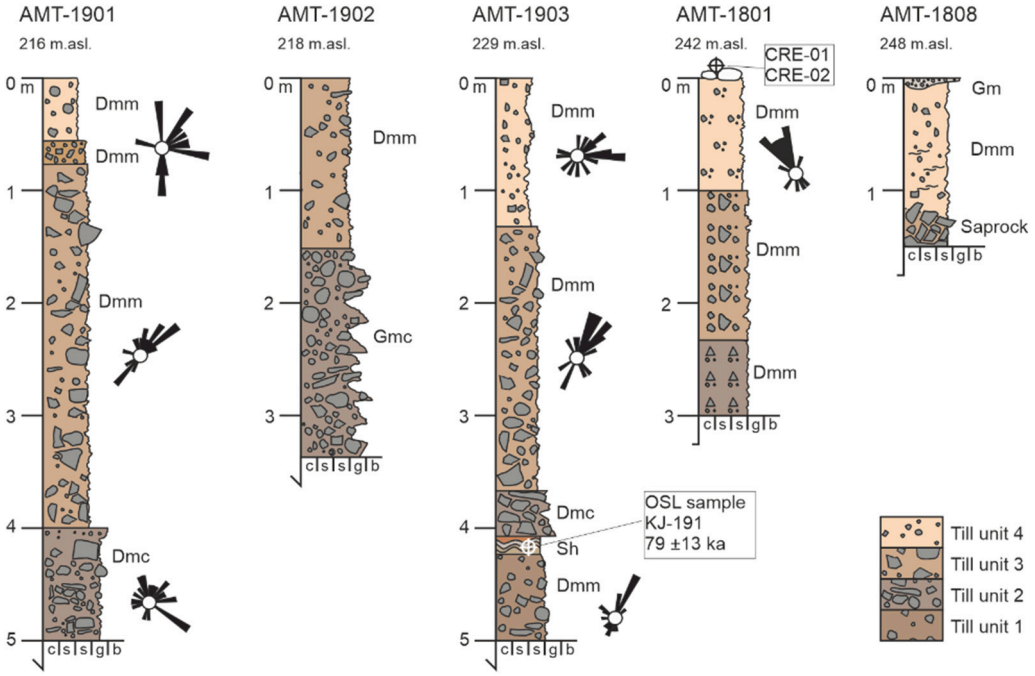

Fig. 5. Kaarestunturi sediment stratigraphy. Stratigraphy logs are drawn from machine cut trenches AMT-1801 to AMT-1903 south and southeast of Kaarestunturi fell. For locations, see Fig. 2.

diamicton. The unit composes of a sandy matrix and approximately 20 % clasts. Clasts mode is in the pebble size range. The fabric calculations produce incoherent and inconsistent rose diagrams, they were measured in AMT-1903 and AMT-1801.

4.4. Mineralized erratics at the study site

The mineralized erratics indicate potential for near-surface gold mineralization in the region. The undiscovered mineralization is hosted in a quartz vein system that is likely buried under sediments. The discovered quartz erratics are found both indiscriminately around the study area and in dense NNW-SSE orientated trains (Fig. 2A). The recorded erratic volumes are larger in the NNW parts of the trains and decrease towards the SSE. The apparent spatial distribution is possible partly biased by human sampling. Erratic sampling creates spatial false negatives in highly vegetated and in peatland areas where the mineral sediment is difficult to observe. False positive erratic occurrences are very unlikely.

5. Discussion

Mineral exploration in glaciated regions is typically concerned with the most recent glaciation (e.g., McClenaghan et al., 2000) and the associated ice-flow direction. This is often sufficient and can lead to successful tracing campaigns, but there are scenarios where earlier glaciations play a role in geochemical mineral exploration (Parent et al., 1996). In this study the TCN ages of the dated erratics precede the latest glaciation, showing that the samples have been exposed in an earlier ice-free event. The stratigraphic investigations from the trenches AMT-1801 to AMT-1903 identify a complex and well-preserved stratigraphy. This alongside the well preserved bedrock TCN inventories indicate weakly erosive and repeatedly glaciated area. The observations are in line with earlier studies (e.g., Salonen, 1986; Hirvas and Nenonen, 1990; Stroeven et al., 2002) and suggests that mineral exploration should consider the possibility of reworking of till material.

5.1. The Weichselian glacial cycle in the study area

Kaarestunturi area hosts at least four till units (Fig. 5), as is typical in the region (Hirvas, 1991). The oldest till unit (TU-1) is located below the sand unit dated at 79 ± 13 ka (MIS-5a) using OSL and the till unit therefore likely represents a glaciation during MIS-5b or earlier. The TU-2 till corresponds to a younger glacial event between MIS-4 and MIS-2, thereafter, possibly signaling the presence of the middle Weichselian glaciation. The TU-3 unit likely corresponds to the Late Weichselian advance in MIS-2 in the Sodankylä region and the "Till Unit II" of Hirvas (1991). The uppermost TU-4 is interpreted to be a Late Weichselian deglaciation ablation till. The KJ-191 OSL age of 79 ± 13 ka can constrain the ages of TU-2 and TU-1 chronologically, but the correlation of these older till units with known glacial events remains ambiguous (Åberg et al., 2020).

The generalized ice-flow directions during the aforementioned glaciations are: NW-SE in the Early- (MIS-5b/5d) and Middle Weichselian (MIS-4), W-E in Late Weichselian (MIS-2) and topographically controlled and discordant in the Late Weichselian deglaciation (MIS-2) (Hirvas, 1991; Kleman et al., 1997; Johansson, 1998; Salonen et al., 2014; Lunkka et al., 2015). The results of this study, alongside those of from a nearby study (Härkönen et al., 1981), suggest a SW-NE local ice flow direction in the late-Weichselian glaciation (MIS-2).

5.2. Glacial erosion in the study area

The apparent TCN ages of 53.0 ± 1.8 ka (367 m a.s.l.) and 98.0 ± 2.8 (226 m a.s.l.) from bedrock samples CRE-03 and CRE-04 (Table 4) are considerably old. The apparent ages are comparable to or older than those in nearby tors (55.8 ka and 89.1 ka) (Darmody et al., 2008). However, the highly decayed $^{26}Al/^{10}Be$ ratios (4.7–5.3) in Darmody et al. (2008) show that the tors have been exposed much longer overall – the exposure has been interpreted to span over 14–16 glaciations. The $^{26}Al/^{10}Be$ ratios (6.3–7.0) at Kaarestunturi are higher, showing that although similarly in apparent age, the TCN inventories at Kaarestunturi are younger than the tors in the region. However, the TCN inventories of CRE-03 and CRE-04 presumably also formed in complex sequences of exposures and burials. Together with the well-preserved complex stratigraphy, the TCN results suggests weak glacial erosion and cold based conditions with sluggish ice movement and consequentially, short glacial transportation distances (Waller, 2001; Näslund et al., 2003; Hall et al., 2015). Weak erosion would mean that the mineralized erratics have been mobilized by shallow erosion of near-surface bedrock. Although the study area has not experienced pervasive erosion in recent glaciations in general (Ebert et al., 2015), trench AMT-1808 (Fig. 2) may document a location where recent erosion has been stronger. The stratigraphy for this trench is comprised solely of the TU-4 unit (Fig. 5), with no older preserved till beds. This could suggest that the site experienced topographically steered, limited erosion during the most recent deglaciation (feature also reported by Hirvas (1991)).

5.3. Erratic exposure and inheritance in the TCN inventories

The apparent TCN ages of the erratics (39.2 ± 1.3 ka and 30.6 ± 1.0 ka, Table 4) predate the current ice-free period, which can only account for approximately 10.4 ka (Stroeven et al., 2016) of the exposure age of the samples. Thus, the TCN ages contain inheritance from exposure during one or more earlier ice-free periods. This means that multi-staged glacial transportation of the erratics is possible in the study area, although not required. It is also possible that the samples were eroded from bedrock with similar TCN inventories. In this case, multi-staged transportation would not have been required to produce the large TCN inventories. However, even in a near surface vertical vein system, the surrounding wall rock would shield the veins from most of the radiation (Fig. 3) meaning that accumulating significant amounts of TCNs would take a long time. This could be the case with CRE-01, whose $^{26}Al/^{10}Be$ ratio is disproportionally depleted, however, same does not apply to CRE-02 (Table 3). Ultimately the proportions of accumulated TCNs are difficult to define, and it is possible that the inventories compose of nuclides attained both as a part of bedrock and as mobile erratics.

5.4. Linking the TCN ages to the glacial history of the study area

Thick continental glaciers shield the ground surface from most of the cosmogenic radiation flux and, in practice, interrupt the accumulation of TCN in shielded samples during these periods (Fig. 3, (Gosse and Phillips, 2001)). This means that during local glaciations TNCs are not produced in the samples and the time periods are not included in the apparent age of the samples. Here we include the glaciations *ex post* with the assumption that they have been sufficiently thick (>35 m, see e.g., Miller et al. (2006)) to shield the samples from most of the radiation flux. By projecting the apparent exposure ages against a local glacial shielding model, the TCN ages portray a chronological image that includes glaciations (Fig. 6) and allows estimations on initial exposure events or on erosion events of corresponding samples. However, the estimations are limited by the accuracy of the interpreted shielding history. The current knowledge of past glacier extents and thicknesses in the study area are limited, making the interpreted shielding conditions tentative. The provided interpretation of glacial shielding at the study site (Fig. 6) is primarily rooted in regional OSL and ^{14}C dating results (Nydal et al., 1970, Heikkinen et al., 1974, Hirvas and Kujansuu, 1979, Jungner, 1979, Hirvas, 1991, Hirvas et al., 1981, Helmens et al., 2000, Sarala and Eskola, 2011, Åberg et al., 2020, Table 2.) and is influenced by e.g. Johansson et al. (2011). The most recent MIS-2 glaciation is relatively well studied (Hughes et al., 2016, and references therein) but the extents and durations of the older glaciations are still under debate (Helmens

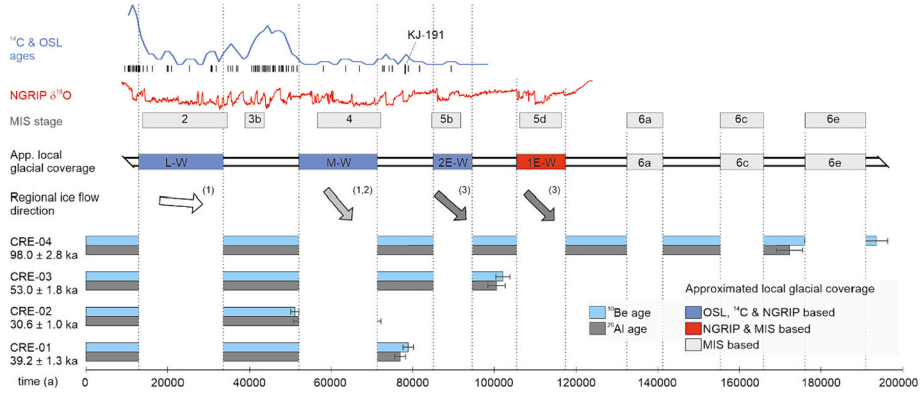

Fig. 6. A glacial shielding model for the Kaarestunturi study area. Approximated local glacial coverage history of the study area and accordingly modelled TCN-samples (Table 4). Apparent TCN ages from Kaarestunturi plotted against a glacial history model of the area. Glaciated periods are interpreted from ^{14}C and OSL ages, NGRIP- and MIS-records. ^{14}C and OSL ages are sourced from Nydal et al. (1970), Heikkinen et al. (1974), Hirvas and Kujansuu (1979), Jungner (1979), Hirvas et al. (1981), Hirvas (1991), Helmens et al. (2000), Sarala and Eskola (2011), Åberg et al. (2020) and Table 2. between latitudes 67° and 68° in Finnish Lapland. Each dating is presented with a tick on the x-axis and the blue line plots their frequency. The NGRIP δ^{18}O record follows Kindler et al. (2014) and the MIS-record the interpretation of Railsback et al. (2015). Ice flow directions from 1: Hirvas (1991) 2: Härkönen et al. (1981), Salonen et al. (2014), Åberg et al. (2020) and 3: Lunkka et al. (2015), Sutinen and Middleton (2021).

Table 2
OSL sample information from trench AMT-1903.

Sample	Laboratory no.	Trench	Municipality	Latitude (DD)	Longitude (DD)	Material	Eq. Dose (Gy)	Age (ka)	Year
KJ-191	Hel-TL04350	AMT-1903	Sodankylä	67.5519	26.2993	sand	166 ± 15	79 ± 13	2019

and Engels, 2010; Salonen et al., 2014). Our model is most accurate within the timespan that is supported by sedimentary dating results (Fig. 6) and is gradually less accurate with the growing uncertainty linked to historical glacier thicknesses and extents.

The glacial shielding model (Fig. 6) suggests that the CRE-01 and CRE-02 erratics were exposed prior to the Middle Weichselian (MIS-4) glaciation and in the Middle Weichselian glaciation, respectively. The ^{26}Al/^{10}Be ratio of CRE-01 is smaller than the one of CRE-02 (Fig. 7). The ratio discrepancy between the erratics suggests longer reburial for CRE-01. This would mean that the time difference between the initial exposure events of the sampled erratics is larger than what the apparent ages lead to believe. However, the overlapping ratio error bars facilitate only speculation. When projected on the glacial shielding model (Fig. 6) the apparent age of CRE-02 suggests it was eroded in MIS-4 glaciation and was first exposed at the following deglaciation. CRE-01 in turn may have been eroded and first exposed some time in MIS-5, possibly containing a reburial effect (Heyman et al., 2011) and a smaller ^{26}Al/^{10}Be ratio. The near coevality of the boulder samples may indicate that they were exposed in event-like erosion. The boulder TCN samples are not only diagnostic to the transportation history boulders but should also apply to their source. At Kaarestunturi the boulders relay that the mineralization was close enough to the surface to be eroded and irradiated already much prior to the latest glaciation. Constraining the timing of the minimum initial exposure event from the erratics is important for provenance tracing because it places boundaries on the time window when the host deposit first met the erosive plane. These boundaries can define the time window when first crystalline geochemical indicators of the deposit may have been released into the surface sediment and help in tracing their origin (Bouchard and Salonen, 1990). Bedrock samples on the other hand provide mineral exploration with information of the local erosion depth and age.

5.5. *Reconstructing transportation paths for the mineralized erratics*

The mobilized, mineralized glacial erratics form a 3-km-long SSE dissipating fan. The volume of the erratics is higher in the NNW, implying that it is proximal to the source of the Au mineralization. The majority of quartz boulders at the site are deposited on top of the MIS-2 ablation till (TU-4) and the corresponding glacial event therefore likely played a role in their displacement. The TCN results show that the dated erratics (CRE-1 and -02) were initially exposed earlier, therefore their transportation possibly started prior to the MIS-2 glaciation (Fig. 6). At the same time, the in-situ bedrock samples CRE-03 and CRE-04 document weak glacial erosion, suggesting that the glacial movement and transportation has been weak at the area during recent glaciations.

Due to the strong stratigraphic association of the erratics with the surface of the TU-4 unit, it is likely that the erratics melted out from a relatively clean ice column. Debris poor ice could have been sourced from the fell during deglaciation. The implied short transportation would also be consistent with the large size of the erratics (Bouchard and Salonen, 1990) and the shape and distribution of the fan (Boulton, 1978) (Fig. 2). The apparent absence of quartz boulders in older till units suggests that the quartz boulders may not have located in the valley prior to the deglaciation, at least in large numbers. Considering this, Fig. 8 shows the interpreted *syn*-LGM position of the proto erratics in their positions that most likely preceded the MIS-2 deglaciation related

Table 3
TCN sample analytical results and ages. Ages are presented with St scaling scheme (Stone, 2000) without erosion or snow shielding.

Sample	Quartz used (g)	^{10}Be (at g-1)	Exposure age ^{10}Be (ka)	^{26}Al (at g-1)	Exposure age ^{26}Al (ka)	^{26}Al/^{10}Be ratio
CRE-01	20.4191	2.00E+05	37.8 ± 1.2	1,293,287	35.9 ± 1.3	6.48 ± 0.31
CRE-02	20.0738	1.56E+05	29.5 ± 1.0	1,096,365	30.3 ± 1.1	7.01 ± 0.33
CRE-03	20.1436	2.99E+05	50.3 ± 1.6	1,973,220	48.9 ± 1.9	6.60 ± 0.33
CRE-04	20.0979	4.63E+05	91.0 ± 2.4	2,926,864	85.3 ± 2.8	6.32 ± 0.26

Table 4
Results recalculated with snow shielding and erosion rates. Ages are presented with St scaling scheme (Stone, 2000).

Sample	Snow compensated sample thickness (cm)	Erosion rate mm ka-1	Nuclide, mineral	^{10}Be exposure age (int error)	Nuclide, mineral	^{26}Al exposure age (int error)
CRE-01	7.98	0.5	Be-10, quartz	39.2 ± 1.3 ka	Al-26, quartz	37.2 ± 1.4 ka
CRE-02	7.98	0.5	Be-10, quartz	30.6 ± 1.0 ka	Al-26, quartz	31.4 ± 1.2 ka
CRE-03	6.19	0.9	Be-10, quartz	53.0 ± 1.8 ka	Al-26, quartz	51.4 ± 2.2 ka
CRE-04	7.91	0.7	Be-10, quartz	98.0 ± 2.8 ka	Al-26, quartz	91.6 ± 3.3 ka

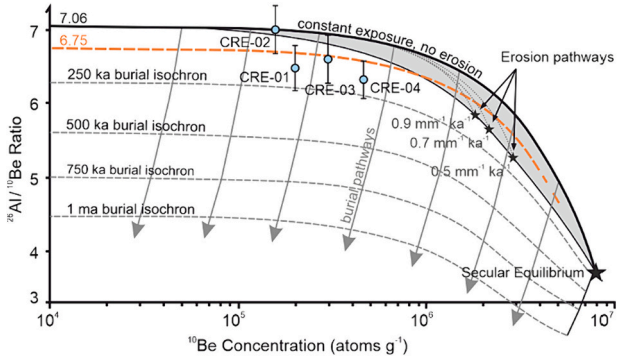

Fig. 7. An estimation of sample reburial with a ^{26}Al/^{10}Be ratio plot, edited from Corbett et al. (2013) and Dehnert and Schlüchter (2008). The plot illustrates sample reburial through the decay of corresponding ^{26}Al/^{10}Be ratios. Due to the differing half-lives of ^{26}Al and ^{10}Be their ratio declines if a sample is reburied after an exposure event. The commonly cited ratio of 6.75 is present for reference, but it plots most of CRE-02 outside the possible region. In the absence of a local production rate ratio, the CRE-02's ^{26}Al/^{10}Be = 7.01 (Table 3) is used as the minimum production rate ratio and the constant exposure curve is set to start at 7.06 which accommodates CRE-02 on the "constant exposure" line. However, the sample predates the MIS-2 glaciation (Fig. 6) and its ^{26}Al/^{10}Be ratio can therefore be expected to being slightly depleted.

displacement.

The modelled TCN ages plot the minimum initial surfacing of samples CRE-01 and CRE-02 to the Middle- (MIS-4) and Early Weichselian (MIS-5b/5d) glaciations (Figs. 6, 7). In Fig. 9, a tentative pre-LGM probability sector is defined using the regional ice flow directions after the interpreted minimum initial exposure of the erratic samples. The directions are sourced both from the results of this study (Fig. 5) and from literature (Härkönen et al., 1981; Hirvas, 1991; Kleman et al., 1997; Johansson, 1998; Salonen et al., 2014; Lunkka et al., 2015; Åberg et al., 2020; Sutinen and Middleton, 2021). The similar Middle- and Early Weichselian ice-flow directions are presented together (Åberg et al., 2020).

The produced probability sector suggests that the deposit lays NWW from the current location of the dated CRE-01 and CRE-02 erratics. The right boundary of the NWW pointing sector is based on the indicated Middle- and Early-Weichselian ice flow directions, adjusted with the possibility of topographic steering of ice by the fell. The left boundary of the sector is from the locally measured TU-3 till fabric that we interpret to show ice flow during the late-Weichselian glaciation. The "inferred priority area" further constrains the area, only using the recent late Weichselian glacial events. The area assumes a singular source for the erratics, near the apex of the erratic train. The area comprises the syn-LGM position from Fig. 8 adjusted by the prominent late-Weichselian ice-flow direction observed in the till unit TU-3.

Although the tracing results of this study can be viewed in their entirety, from mineral exploration point of view it is more beneficial to view them as chronological sequence of possible displacement events, as displacement in all of the indicated events is not guaranteed. Because the events are conceptualized separately in the study, they can be traced separately as well. This allows emphasizing or disregarding particular transportation events according to new observations on site.

6. Applicability of TCN-dating in exploration

Indicator tracing in glacial domains generally uses the exponential sediment dispersal function described in Krumbein (1937) to trace geochemical or erratic fans back to their source (Puranen, 1988; Nurmi, 1991). However, tracing campaigns that rely on the simple dispersal model in a complex glacial setting can be erroneous as a result of incorrect till interpretation, a multi-staged transportation history, or reworking of till material (Saksela, 1948; Salonen, 1986; Levson and Giles, 1995). The use of TCN dating, especially when accompanied by stratigraphic studies has the potential to reduce such uncertainties in exploration. TCN dating characterizes erosion and its depth, producing minimum ages for local erosion events (Fig. 6). The results can be used to infer various things such as the expected number of stages of transportation, the transport directions and distance, or the size of the source area. The practical benefits of the method in the field are that (1) it is suitable for most quartz-bearing rock types, (2) collecting the 0.5 to 1 kg samples is fast and can be conducted in locations that are difficult to access or remote, (3) the method can produce valuable results even with a small number of samples, and 4) the method has a very low environmental impact and a survey can be conducted with light exploration permits (Gosse and Phillips, 2001). In contrast, however, the measurement cost and up to one year sample processing times limit the widespread use of the method.

When working with erratics, this method can identify whether a multi-stage transportation history is possible based on the measured TCN inventory. Although multi-stage transportation is well known (Parent et al., 1996), it can most often only be recognized in hindsight after analyzing the quantities of geochemical assays. If the apparent ages based on TCN inventories significantly predate deglaciation or show strong decay in the ^{26}Al/^{10}Be ratios, the erratics or their source area has experienced prior exposure. Prior exposure means that the erratic or its source area has been on the surface or in near-surface conditions prior to the latest glaciation. In glaciated regions, this would suggest multiple stages of transportation are possible.

In the case of geochemical or heavy mineral anomalies, the local glacial transportation distances can be characterized from the TCN inventories of local bedrock sites. The results apply similarly to erratic anomalies. Large inheritance in TCN inventories is indicative of weak glacial erosion and short transportation. Weak erosion is also likely to preserve pre-existing sediments (Ebert et al., 2015), which in its turn is an environment where till recycling is more prominent (Finck and Stea, 1995). This is important because till recycling can imprint historical transportation directions on a boulder train and its geochemical anomaly (Salonen, 1986; Parent et al., 1996). Preservation of sediment strata also puts a strong emphasis on which superimposed till unit the till survey intercepts (Lunkka et al., 2013). In the case of sub surface sampling (e.g. base of till), it is possible to intercept e.g. interbedded or basal

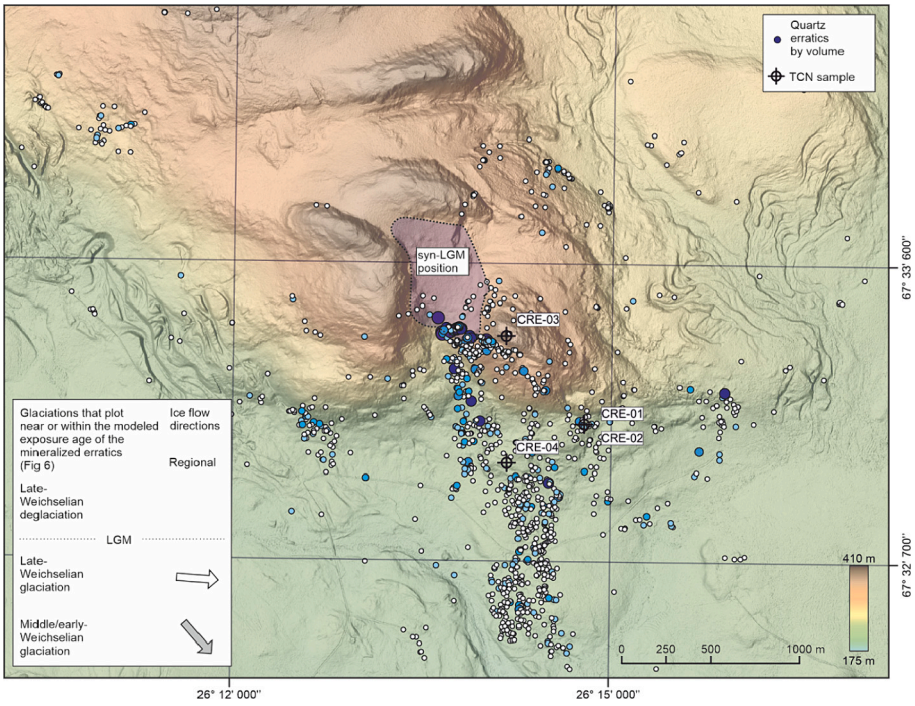

Fig. 8. Interpreted syn-last glacial maximum (LGM) positions of the proto quartz erratics. The indicated syn-LGM location assumes that the CRE-01 and CRE-02 erratics are a part of the dispersal fan. The transportation directions are based on literature (see Fig. 6), for erratic volume legend see Fig. 2. LiDAR DEM: © modified and reproduced after the National Land Survey of Finland, accessed on 1 December 2022.

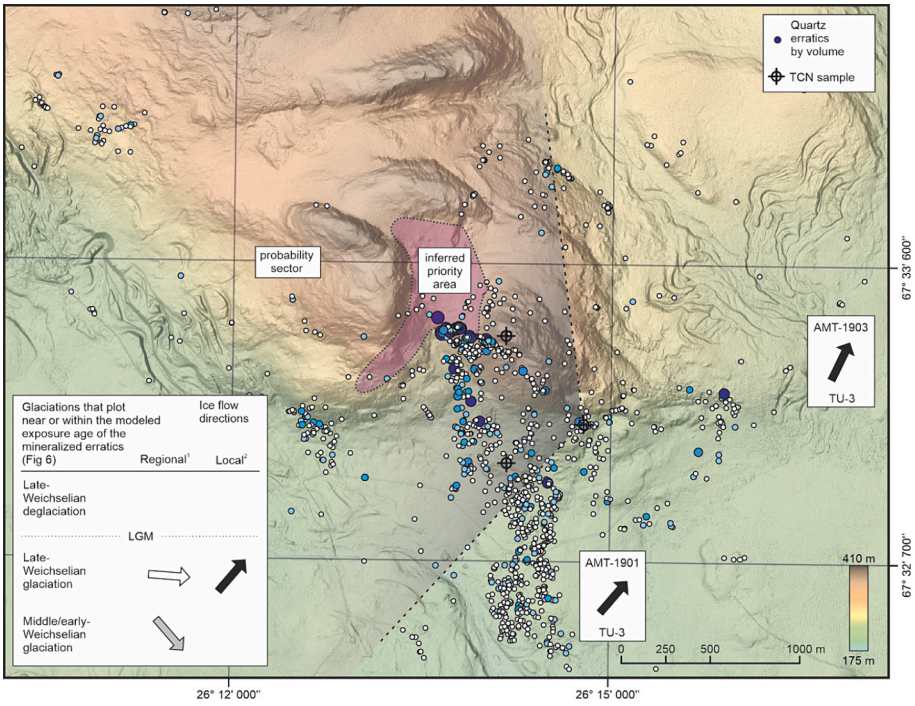

Fig. 9. A Tentative probability sector and inferred priority area for the erratic source. The sector is interpreted by applying transportation directions from Fig. 6 on the CRE-01 and -02 erratics. The glacial events are picked according to the modelled exposure and reburial histories of the erratics (Figs. 7, 6). The transportation directions are based on literature [(1)] (Hirvas, 1991; Åberg et al., 2020) and local studies [(2)] (Fig. 5). The inferred priority area is based on indicated weak erosion and prolonged exposure of the dated erratics (Fig. 5, Table 4). For erratic volume legend see Fig. 2. LiDAR DEM: © modified and reproduced after the National Land Survey of Finland, accessed on 1 December 2022.

gravels (Hirvas, 1991). These sediments can be anomalous for placer gold, giving out a false positive result for the till survey.

In areas with greater erosion magnitudes, TCN inventories can be used to identify *event surfaces* (Phillips et al., 2006), which form after pervasive erosion events remove most of the TCN inventory of an outcrop (Fig. 3). In the glacial erosion context event surfaces can record

the most recent highly erosive glacial event in the area. TCN inventories that are either modelled (Fig. 6) or directly analyzed from these surfaces record the timing of the deglaciation that followed the highly erosive glacial event. Because highly erosive glacial events also typically erode pre-existing sediments, event surfaces can provide indirect information about the age and complexity of regional stratigraphy. The consistent presence of young event surfaces in an exploration region can bolster confidence in geochemical surveys, while also suggesting that the most prominent glacial displacement direction that affected the geochemical tracers has been the most recent one. In contrast, the lack of young event surface in a region, would suggest that care should be taken in all geochemical assay interpretations in the manner that this paper describes.

7. Conclusions

At Kaarestunturi the TCN inventories show prolonged exposure to cosmogenic radiation that is consistent with multi-staged transportation, repeated exposure in the source area, or both. Together the TCN results and stratigraphic investigations contain an exposure and erosion history over 100 ka, the preservation of which is a sign of weak glacial erosion at the study area during this time interval. Low erosion rates below cold-based ice imply short distances of transport for till material and boulders, suggesting the source area is proximal to the erratics. The combined TCN results and stratigraphic studies suggest a SSW-N bounded probability sector for the host deposit.

TCN dating can contribute to exploration campaigns by reducing the uncertainty involved in till-based sampling and by enabling pre-emptive measures in selecting the optimal exploration methods, for example. The benefits of TCN inventory measurements using ^{26}Al and ^{10}Be are:

- The survey can characterize and date erosion events and depth of erosion. Strong glacial erosion will remove pre-existing sediments and palimpsests, simplifying the interpretation of geochemical samples. In contrast, evidence of weak glacial erosion can indicate the geochemical data interpretation may be more complex.
- By discovering direct or modelled event surfaces from TCN inventories, exploration can identify most relevant local transportation directions or implied palimpsests of historical directions.
- In some cases, transportation distances can be inferred from the strength of erosion. Cold-based weakly erosive glacial settings imply short transportation.
- From TCN inventories of erratics, it is possible to evaluate possibility of multi-phase transportation and possible periods of burial.
- The TCN method is a geomorphological dating tool and provides basic research value for exploration campaigns.

Including TCN inventory measurements can ultimately help in reducing uncertainty when identifying possible source areas for geochemical tracers. It is particularly helpful in weakly erosive regions where these uncertainties are largest.

Declaration of competing interest

The authors declare the following financial interests/personal relationships which may be considered as potential competing interests. Veikko Peltonen reports financial support was provided by K H Renlund Foundation.

Data availability

The authors do not have permission to share data.

Acknowledgements

The study was funded by the K.H. Renlund Foundation. For their cooperation we thank the companies Aurion Resources LTD and Firefox Gold and The ASTER AMS national facility (CEREGE, Aix-en-Provence) supported by the INSU/CNRS, the ANR through the “Projets thematiques d'excellence” program for the “Equipements d'excellence” ASTER-CEREGE action and IRD. For their work in proof reading and commenting we thank Jaakko Georgi, Viveka Laakso, Juuso Uusikorpi, Saara Silvennoinen, Oscar Wilson and others who helped in the writing of this manuscript. We thank the anonymous reviewer for their work and their comments that helped in improving the manuscript.

References

Aario, R., Peuraniemi, V., 1992. Glacial dispersal of till constituents in morainic landforms of different types. Geomorphology 6 (1), 9–25.
Åberg, A.K., Kultti, S., Kaakinen, A., Eskola, K.O., Salonen, V.-P., 2020. Weichselian sedimentary record and ice-flow patterns in the Sodankylä area, central Finnish Lapland. Bull. Geol. Soc. Finl. 92 (1–2), 77.
Aitken, M.J., 1985. Thermoluminescence dating: past progress and future trends. Nuclear Tracks Radiation Measurements 10 (1–2), 3–6.
Andersen, J.L., Egholm, D.L., Olsen, J., Larsen, N.K., Knudsen, M.F.J.E., Letters, P.S., 2020. Topographical evolution and glaciation history of South Greenland constrained by paired 26Al/10Be nuclides 542, 116300.
Argento, D.C., Stone, J.O., Reedy, R.C., O'Brien, K., 2015. Physics-based modeling of cosmogenic nuclides part II–key aspects of in-situ cosmogenic nuclide production. Quat. Geochronol. 26, 44–55.
Arnold, M., Merchel, S., Bourlès, D.L., Braucher, R., Benedetti, L., Finkel, R.C., Aumaître, G., Gottdang, A., Klein, M., 2010. The French accelerator mass spectrometry facility ASTER: improved performance and developments. Nucl. Instrum. Methods Phys. Res., Sect. B 268 (11−12), 1954–1959.
Balco, G., Stone, J.O., Lifton, N.A., Dunai, T.J., 2008. A complete and easily accessible means of calculating surface exposure ages or erosion rates from Be-10 and Al-26 measurements. Quat. Geochronol. 3 (3), 174–195.
Balco, G., Stone, J.O.H., Sliwinski, M.G., Todd, C., 2014. Features of the glacial history of the Transantarctic Mountains inferred from cosmogenic Al-26, Be-10 and Ne-21 concentrations in bedrock surfaces. Antarct. Sci. 26 (6), 708–723.
Bierman, P.R., Marsella, K.A., Patterson, C., Davis, P.T., Caffee, M., 1999. Mid-Pleistocene cosmogenic minimum-age limits for pre-Wisconsinan glacial surfaces in southwestern Minnesota and southern Baffin Island; a multiple nuclide approach. Geomorphology 27 (1–2), 25–39.
Borchers, B., Marrero, S., Balco, G., Caffee, M., Goehring, B., Lifton, N., Nishiizumi, K., Phillips, F., Schaefer, J., Stone, J., 2016. Geological calibration of spallation production rates in the CRONUS-Earth project. Quat. Geochronol. 31, 188–198.
Bøtter-Jensen, L., Duller, G., 1992. A new system for measuring optically stimulated luminescence from quartz samples. International Journal of Radiation Applications and Instrumentation 20 (4), 549–553.
Bøtter-Jensen, L., Duller, G., Murray, A., Banerjee, D., 1999. Blue light emitting diodes for optical stimulation of quartz in retrospective dosimetry and dating. Radiat. Prot. Dosim. 84 (1–4), 335–340.
Bouchard, M., Salonen, V.-P., 1990. Boulder transport in shield areas. Glacial Indicator Tracing 87–107.
Boulton, G.S., 1978. Boulder shapes and grain-size distributions of debris as indicators of transport paths through a glacier and till genesis. Sedimentology 25 (6), 773–799.
Bradshaw, P.M., Thomson, I., Smee, B.W., Larsson, J.O.J.J., o. G. E., 1974. The application of different analytical extractions and soil profile sampling in exploration geochemistry. 3 (3), 209–225.
Child, D., Elliott, G., Mifsud, C., Smith, A.M., Fink, D., 2000. Sample processing for earth science studies at ANTARES. Nuclear Instruments & Methods in Physics Research Section B-Beam Interactions with Materials and Atoms 172, 856–860.
Chmeleff, J., von Blanckenburg, F., Kossert, K., Jakob, D., 2010. Determination of the ^{10}Be half-life by multicollector ICP-MS and liquid scintillation counting. Nucl. Instrum. Methods Phys. Res., Sect. B 268 (2), 192–199.
Corbett, L.B., Bierman, P.R., Graly, J.A., Neumann, T.A., Rood, D.H.J.B., 2013. Constraining landscape history and glacial erosivity using paired cosmogenic nuclides in Upernavik, northwest Greenland. 125 (9–10), 1539–1553.
Corbett, L.B., Bierman, P.R., Rood, D.H., Caffee, M.W., Lifton, N.A., Woodruff, T.E., 2017. Cosmogenic ^{26}Al/^{10}Be surface production ratio in Greenland. Geophys. Res. Lett. 44 (3), 1350–1359.
Darmody, R.G., Thorn, C.E., Seppälä, M., Campbell, S.W., Li, Y.K., Harbor, J., 2008. Age and weathering status of granite tors in Arctic Finland (~68° N). Geomorphology 94 (1–2), 10–23.
Davis Jr., R., Schaeffer, O.A., 1955. Chlorine-36 in nature. Ann. N. Y. Acad. Sci. 62 (5), 107–121.
Dehnert, A., Schlüchter, C., 2008. Sediment burial dating using terrestrial cosmogenic nuclides. Quat. Sci. J. 57 (1/2), 210–225.
DiLabio, R.N.W., 1990. Glacial dispersal trains. CRC Press, Glacial indicator tracing, pp. 109–122.
Dunai, T.J., 2010. Cosmogenic Nuclides: Principles, Concepts and Applications in the Earth Surface Sciences. Cambridge University Press, Cambridge.
Ebert, K., Hall, A.M., Kleman, J., Andersson, J., 2015. Unequal ice-sheet erosional impacts across low-relief shield terrain in northern Fennoscandia. Geomorphology 233, 64–74.

Eyles, N., Eyles, C.H., Miall, A.D., 1983. Lithofacies types and vertical profile models; an alternative approach to the description and environmental interpretation of glacial diamict and diamictite sequences. Sedimentology 30 (3), 393–410.
Finck, P.W., Stea, R.R., 1995. The compositional development of tills overlying the South Mountain Batholith. Nova Scotia. Energy Mines Energy Branches Paper 95, 91.
Gosse, J.C., Phillips, F.M., 2001. Terrestrial in situ cosmogenic nuclides: theory and application. Quat. Sci. Rev. 20 (14), 1475–1560.
Granger, D.E., Muzikar, P.F., 2001. Dating sediment burial with in situ-produced cosmogenic nuclides: theory, techniques, and limitations. Earth Planet. Sci. Lett. 188 (1–2), 269–281.
Hall, A.M., Sarala, P., Ebert, K., 2015. Late Cenozoic deep weathering patterns on the Fennoscandian shield in northern Finland: a window on ice sheet bed conditions at the onset of Northern Hemisphere glaciation. Geomorphology 246, 472–488.
Hall, A.M., Ebert, K., Goodfellow, B.W., Hattestrand, C., Heyman, J., Krabbendam, M., Moon, S., Stroeven, A.P., 2019. Past and Future Impact of Glacial erosion in Forsmark and Uppland. Final report, Svensk Kambranslehantering, p. 247.
Härkönen, I., Pulkkinen, E., Lindroos, P., 1981. Eräiden mineralisaatioiden kuvastuminen pintamoreenissa Keski-Lapissa. Report of Investigation, Geologinen tutkimuslaitos. 55, 53–59.
Heikkinen, A., Koivisto, A.-K., Aikaa, O., 1974. Geological survey of Finland radiocarbon measurements VI. Radiocarbon 16 (2), 252–268.
Helmens, K.F., Engels, S.J., 2010. Ice-free conditions in eastern Fennoscandia during early Marine Isotope Stage 3: lacustrine records. Boreas 39 (2), 399–409.
Helmens, K.F., Räsänen, M.E., Johansson, P.W., Jungner, H., Korjonen, K.J., 2000. The last interglacial-glacial cycle in NE Fennoscandia: a nearly continuous record from Sokli (Finnish Lapland). Quat. Sci. Rev. 19 (16), 1605–1623.
Heyman, J., Stroeven, A.P., Harbor, J.M., Caffee, M.W., 2011. Too young or too old: evaluating cosmogenic exposure dating based on an analysis of compiled boulder exposure ages. Earth Planet. Sci. Lett. 302 (1–2), 71–80.
Hilger, P., Gosse, J.C., Hermanns, R.L., 2019. How significant is inheritance when dating rockslide boulders with terrestrial cosmogenic nuclide dating?—a case study of an historic event. Landslides 16 (4), 729–738.
Hirvas, H., 1991. Pleistocene stratigraphy of Finnish Lapland. Bull. Geol. Soc. Finl. 354, 123.
Hirvas, H., Kujansuu, R., 1979. On glacial, interstadial and interglacial deposits in Northern Finland. IGCP Project 73 (1), 24.
Hirvas, H., Nenonen, K., 1990. Field methods for glacial indicator tracing. Glacial Indicator Tracing 217–248.
Hirvas, H., Alfthan, A., Pulkkinen, E., Puranen, R., Tynni, R., 1977. A report on glacial drift investigations for one prospecting purposes in northern Finland 1972-1976. Report of Investigation, Geologinen tutkimuslaitos. 19, 54.
Hirvas, H., Korpela, K., Kujansuu, R., 1981. Weichselian in Finland before 15,000 Bp. Boreas 10 (4), 423–431.
Hughes, A.L.C., Gyllencreutz, R., Lohne, O.S., Mangerud, J., Svendsen, J.I., 2016. The last Eurasian ice sheets - a chronological database and time-slice reconstruction, DATED-1. Boreas 45 (1), 1–45.
Johansson, P., 1998. The Deglaciation in Eastern Part of the Weichselian Ice Divide in Finnish Lapland. University of Turku.
Johansson, P., Lunkka, J.P., Sarala, P., 2011. The Glaciation of Finland. Quaternary Glaciations - Extent and Chronology - A Closer Look 105–116.
Jungner, H., 1979. Radiocarbon dates I. In: Report no. 1. University of Helsinki, Finland, Dating Laboratory.
Kindler, P., Guillevic, M., Baumgartner, M., Schwander, J., Landais, A., Leuenberger, M., 2014. Temperature reconstruction from 10 to 120 kyr b2k from the NGRIP ice core. Clim. Past 10 (2), 887–902.
Klassen, R.A., Gubins, A.G., 1997. Glacial history and ice flow dynamics applied to drift prospecting and geochemical exploration. Proceedings of Exploration 97, 221–232.
Kleman, J., Hättestrand, C., Borgström, I., Stroeven, A., 1997. Fennoscandian palaeoglaciology reconstructed using a glacial geological inversion model. J. Glaciol. 43 (144), 283–299.
Kohl, C., Nishiizumi, K., 1992. Chemical isolation of quartz for measurement of in-situ-produced cosmogenic nuclides. Geochim. Cosmochim. Acta 56 (9), 3583–3587.
Korschinek, G., Bergmaier, A., Faestermann, T., Gerstmann, U.C., Knie, K., Rugel, G., Wallner, A., Dillmann, I., Dollinger, G., von Gostomski, C.L., 2010. A new value for the half-life of ^{10}Be by Heavy-Ion Elastic Recoil Detection and liquid scintillation counting. Nucl. Instrum. Methods Phys. Res., Sect. B 268 (2), 187–191.
Krumbein, W., 1937. Sediments and exponential curves. J. Geol. 45 (6), 577–601.
Lal, D., Peters, B., 1967. Cosmic Ray Produced Radioactivity on the Earth. Springer, Kosmische Strahlung II/Cosmic Rays II, pp. 551–612.
Levson, V.M., Giles, T.R., 1995. Glacial dispersal patterns of mineralized bedrock: with examples from the Nechako Plateau, Central British Columbia. Drift Exploration in the Canadian Cordillera: British Columbia Ministry of Energy, Mines Petroleum Resources Paper 2, 67–76.
Lunkka, J.P., Peuraniemi, V., Nikarmaa, T., 2013. Application of till geochemical and indicator mineral data to the interpretation of the thick till sequence at Muhos, northern Finland. Geochem.: Explor., Environ., Anal. 13 (3), 183–193.
Lunkka, J.P., Sarala, P., Gibbard, P., 2015. The Rautuvaara section, western Finnish Lapland, revisited–new age constraints indicate a complex Scandinavian Ice Sheet history in northern Fennoscandia during the Weichselian Stage. Boreas 44 (1), 68–80.
Margreth, A., Gosse, J., Dyke, A., 2014. Constraining the Timing of Last Glacial Plucking of Tors on Cumberland Peninsula, Baffin Island. Eastern Canadian Arctic, EGU General Assembly Conference Abstracts.
McClenaghan, M.B., Paulen, R.C., 2017. Chapter 20 mineral exploration in glaciated terrain. In: Menzies, J., van der Meer, J.-J.-M. (Eds.), Past Glacial Environments (Sediments, Forms and Techniques), A new & Revised edition. Elsevier, pp. 689–751.
McClenaghan, M.B., Thorleifson, L.H., DiLabio, R.N.W., 2000. Till geochemical and indicator mineral methods in mineral exploration. Ore Geol. Rev. 16 (3–4), 145–166.
Miller, G.H., Briner, J.P., Lifton, N.A., Finkel, R.C., 2006. Limited ice-sheet erosion and complex exposure histories derived from in situ cosmogenic ^{10}Be, ^{26}Al, and ^{14}C on Baffin Island. Arctic Canada. Quaternary Geochronology 1 (1), 74–85.
Näslund, J., Rodhe, L., Fastook, J., Holmlund, P., 2003. New ways of studying ice sheet flow directions and glacial erosion by computer modelling—examples from Fennoscandia. Quat. Sci. Rev. 22 (2–4), 245–258.
Nichol, I., Bjorklund, A., 1973. Glacial geology as a key to geochemical exploration in areas of glacial overburden with particular reference to Canada. J. Geochem. Explor. 2 (2), 133–170.
Niiranen, T., Lahti, I., Nykänen, V., 2015. The Orogenic Gold Potential of the Central Lapland Greenstone Belt, Northern Fennoscandian Shield. Elsevier, Mineral Deposits of Finland, pp. 733–752.
Nishiizumi, K., Imamura, M., Caffee, M.W., Southon, J.R., Finkel, R.C., McAninch, J., 2007. Absolute calibration of Be-10 AMS standards. Nuclear Instruments & Methods in Physics Research Section B-Beam Interactions with Materials and Atoms 258 (2), 403–413.
Nurmi, P.A., 1991. Geological setting, history of discovery and exploration economics of Precambrian gold occurrences in Finland. J. Geochem. Explor. 39 (3), 273–287.
Nydal, R., Loevseth, K., Syrstad, O., 1970. Trondheim natural radiocarbon measurements V. Radiocarbon 12 (1), 205–237.
Parent, M., Paradis, S.J., Doiron, A., 1996. Palimpsest glacial dispersal trains and their significance for drift prospecting. J. Geochem. Explor. 56 (2), 123–140.
Phillips, W.M., Hall, A.M., Mottram, R., Fifield, L.K., Sugden, D.E., 2006. Cosmogenic ^{10}Be and ^{26}Al exposure ages of tors and erratics, Cairngorm Mountains, Scotland: timescales for the development of a classic landscape of selective linear glacial erosion. Geomorphology 73 (3–4), 222–245.
Puranen, R., 1988. Modelling of Glacial Transport of Tills. Glacial indicator Tracing, a.a. Balkema, pp. 15–34.
Railsback, L.B., Gibbard, P.L., Head, M.J., Voarintsoa, N.R.G., Toucanne, S., 2015. An optimized scheme of lettered marine isotope substages for the last 1.0 million years, and the climatostratigraphic nature of isotope stages and substages. Quat. Sci. Rev. 111, 94–106.
Saksela, M., 1948. Outokummun kuparimalmin löytö - the discovery of Outokumpu ore field. In: Geologinen tutkimuslaitos, 47. Geoteknillisiä julkaisuja, p. 36.
Salonen, V.-P., 1986. Glacial transport distance distributions of surface boulders in Finland. Bull. Geol. Soc. Finl. 338, 57.
Salonen, V.-P., Kaakinen, A., Kultti, S., Miettinen, A., Eskola, K.O., Lunkka, J.P., 2008. Middle Weichselian glacial event in the central part of the Scandinavian Ice Sheet recorded in the Hitura pit, Ostrobothnia. Finland. Boreas 37 (1), 38–54.
Salonen, V.-P., Moreau, J., Hyttinen, O., Eskola, K.O., 2014. Mid-Weichselian interstadial in Kolari, western Finnish Lapland. Boreas 43 (3), 627–638.
Sarala, P., Eskola, T., 2011. Middle Weichselian Interstadial deposit in Petäjäselkä. Northern Finland. Quat. Sci. J. 60 (4), 488–492.
Sarala, P., Räisänen, J., Johansson, P., Eskola, K.O., 2015. Aerial LiDAR analysis in geomorphological mapping and geochronological determination of surficial deposits in the Sodankylä region, northern Finland. GFF 137 (4), 293–303.
Schaefer, J.M., Codilean, A.T., Willenbring, J.K., Lu, Z.-T., Keisling, B., Fülöp, R.-H., Val, P., 2022. Cosmogenic nuclide techniques. Nat. Rev. Methods Primers 2 (1), 1–22.
Stone, J.O., 2000. Air pressure and cosmogenic isotope production. J. Geophys. Res. Solid Earth 105 (B10), 23753–23759.
Stroeven, A.P., Fabel, D., Hättestrand, C., Harbor, J., 2002. A relict landscape in the Centre of Fennoscandian glaciation: cosmogenic radionuclide evidence of tors preserved through multiple glacial cycles. Geomorphology 44 (1–2), 145–154.
Stroeven, A.P., Hättestrand, C., Kleman, J., Heyman, J., Fabel, D., Fredin, O., Goodfellow, B.W., Harbor, J.M., Jansen, J.D., Olsen, L., Caffee, M.W., Fink, D., Lundqvist, J., Rosqvist, G.C., Strömberg, B., Jansson, K.N., 2016. Deglaciation of Fennoscandia. Quat. Sci. Rev. 147, 91–121.
Sutinen, R., Middleton, M., 2021. Porttipahta end moraine in Finnish Lapland is constrained to early Weichselian (MIS 5d, Herning stadial). Geomorphology 393, 107942.
Tylmann, K., Rinterknecht, V.R., Woźniak, P.P., Bourlès, D., Schimmelpfennig, I., Guillou, V., Aumaître, G., Keddadouche, K., 2019. The local last Glacial Maximum of the southern Scandinavian Ice Sheet front: Cosmogenic nuclide dating of erratics in northern Poland. Quat. Sci. Rev. 219, 36–46.
Waller, R.I., 2001. The influence of basal processes on the dynamic behaviour of cold-based glaciers. Quat. Int. 86, 117–128.